Relaxation of a strained quantum well at a cleaved surface

Relaxation of a strained quantum well at a cleaved surface

John H. Davies[a)]
Center for Quantized Electronic Structures, University of California, Santa Barbara, California 93106-4170

D. M. Bruls, J. W. A. M. Vugs, and P. M. Koenraad
COBRA Inter-University Research Institute, Department of Physics, Eindhoven University of Technology, P.O. Box 513, NL-5600MB Eindhoven, The Netherlands

(Received 4 October 2001; accepted for publication 18 January 2002)

Scanning probe microscopy of a cleaved semiconductor surface provides a direct measurement of the elastic field of buried, strained structures such as quantum wells or dots, but allowance must be made for relaxation at the surface. We have calculated this relaxation analytically for the exposed edge of a strained quantum well within classical elastic theory for a linear, isotropic, homogeneous medium. The surface bulges outward if the quantum well has a larger natural lattice constant and the dilation changes sign near the surface, which may enhance recombination. Results are given for a well of constant composition or an arbitrary variation along the growth direction and compared with cross-sectional scanning tunneling microscopy of InGaAs quantum wells in GaAs. Consistent values for the composition of the wells were obtained from counting In atoms, x-ray diffraction, and photoluminescence. The lattice constant on the surface and the normal relaxation were compared with the calculation. Qualitative agreement is good but the theory gives only about 80% of the observed displacement. Some of this difference can be explained by the larger size of indium atoms compared with gallium, and the different surface reconstruction and buckling behavior of InAs and GaAs (110) surfaces upon cleavage.
[DOI: 10.1063/1.1459100]

I. INTRODUCTION

Strained heterostructures are widely used in high-performance devices ranging from quantum-well lasers to pseudomorphic field-effect transistors. The strain is homogeneous deep within the mismatched layers of constant thickness used in these structures. In contrast, self-assembled quantum dots generate highly inhomogeneous strain.

A direct approach to study the strain and composition in a sample containing a quantum well or dots is to cleave it and scan the surface with a probe. This can give the composition directly and the strain can be measured in two ways. Subatomic resolution with a scanning tunneling microscope is needed to detect the strain in the plane of the surface.[1,2] Alternatively the distortion normal to the surface can be measured[3,4] because regions under compressive strain bulge outward while tensile strain depresses the surface.[5] This has the advantage that the lateral resolution need only be on the scale of the well or dot, for which atomic force microscopy is sufficient.[3] Unfortunately the measured strain cannot be interpreted directly in terms of an infinite well or buried dot because the material relaxes at the exposed surface to relieve its elastic energy. Similar relaxation occurs at the edge of a wafer containing an otherwise uniform strained layer, or if the edge of the layer is exposed by etching a mesa or quantum pillar.[6]

In Sec. II we present an analytic calculation of the relaxation at a cleaved surface through a mismatched quantum well, such as InGaAs in GaAs. The results are compared with cross-sectional scanning tunneling microscopy in Sec. III. Agreement is generally good but the magnitude of the calculated relaxation is only about 80% of that observed. We consider some possible explanations for this in Sec. IV.

II. THEORY

In this section we describe a simple, analytic method to calculate the relaxation of a strained layer at a surface. The results are also a guide to the relaxation of a partly exposed quantum dot provided that its depth is much larger than its thickness. It is assumed that the elastic response is linear and isotropic, that there are no forces at the surface or interfaces, and that the elastic constants are the same everywhere. All these points are questionable but a more accurate calculation would almost certainly need numerical methods. The structure containing the strained slab is assembled as shown in Fig. 1, following the ''strain suppression'' approach to thermoelasticity.[7,8]

(a) Bring the slab and its two cladding layers nearby without stress. Assume that the lattice constant in the slab exceeds that in the cladding layers by a constant fraction ϵ_0, taken to be positive. The axis z is along the direction of growth, which is now in the plane of the cleaved surface, and y is the outward normal to this surface.

(b) Apply uniform stress of $\sigma_{xx}^{(\mathrm{slab})}=\sigma_{yy}^{(\mathrm{slab})}=-P$ to the edges of the slab to reduce its lattice constant in the xy plane to that of the cladding layers, keeping $\sigma_{zz}^{(\mathrm{slab})}=0$. This re-

a)Permanent address: Department of Electronics and Electrical Engineering, Glasgow University, Glasgow G12 8QQ, Scotland; electronic mail: jdavies@elec.gla.ac.uk

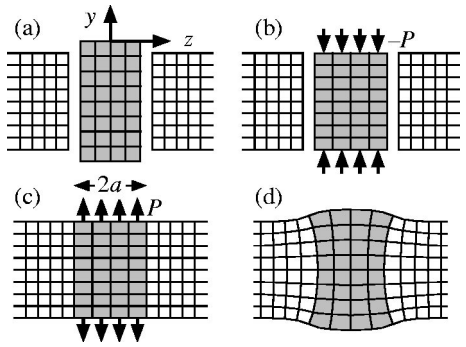

FIG. 1. Construction of elastic problem for a strained quantum well at a surface by "strain suppression." The dimension along y is really much larger than drawn.

quires $P=\epsilon_0 E/(1-\nu)$, where E is Young's modulus and ν is Poisson's ratio. It strains the slab by $\epsilon_{xx}^{(\mathrm{slab})}=\epsilon_{yy}^{(\mathrm{slab})}=-\epsilon_0$ and $\epsilon_{zz}^{(\mathrm{slab})}=2\nu\epsilon_0/(1-\nu)$, with dilation $\epsilon^{(\mathrm{slab})}=-2(1-2\nu)\epsilon_0/(1-\nu)$.

(c) The slab can now be joined to the cladding layers without further strain.

(d) Finally, the fictitious stress applied in the previous step must be canceled by applying an outward pressure of P to the exposed edge of the slab. The region near the surface of both well and cladding layers relaxes under this stress.

It is assumed that the sample is large enough in all dimensions that each exposed edge of the slab can be treated independently. The problem of relaxation then reduces to plane strain with $\epsilon_{xx}^{(\mathrm{rel})}=0$. We need the response of a semi-infinite medium to an applied stress $\sigma_{yy}^{(\mathrm{rel})}(y=0,z)=P$ for $|z|<a$ with no other traction on the surface. This is a standard problem in contact mechanics.[9] The solution shows that the stress obeys $\sigma_{yy}^{(\mathrm{rel})}(0,z)=\sigma_{zz}^{(\mathrm{rel})}(0,z)$ at all points on the surface. It follows immediately that the surface of the cladding layers is unstrained (but not undistorted) and that the surface of the well is uniformly strained by $\epsilon_{zz}^{(\mathrm{rel})}=\epsilon_{yy}^{(\mathrm{rel})}=\epsilon_0(1-2\nu)(1+\nu)/(1-\nu)$. The total strains at the surface of the slab, including the distortion required to match the slab to the cladding, are

$$\epsilon_{xx}=-\epsilon_0, \quad \epsilon_{yy}=\frac{-2\nu^2\epsilon_0}{1-\nu},$$
$$\epsilon_{zz}=(1+2\nu)\epsilon_0, \quad \epsilon=\frac{2\nu(1-2\nu)\epsilon_0}{1-\nu}. \tag{1}$$

These are plotted in Fig. 2(a) for $2a=5$ nm, $\epsilon_0=1\%$, and $\nu=0.31$ (roughly $In_{0.14}Ga_{0.86}As$ in GaAs). The strain ϵ_{yy}, normal to the surface, is reduced by relaxation but ϵ_{zz}, along the direction of growth, *increases* to over 1.6%. This leads to a change in sign of the dilation: it is positive near the surface although the bulk of the slab is in compression.

The displacement $\mathbf{u}(z)$ of the surface is of particular interest because it can be measured with a scanning probe. The component parallel to the surface follows from integration of the strain ϵ_{zz} while the normal component is given by[9]

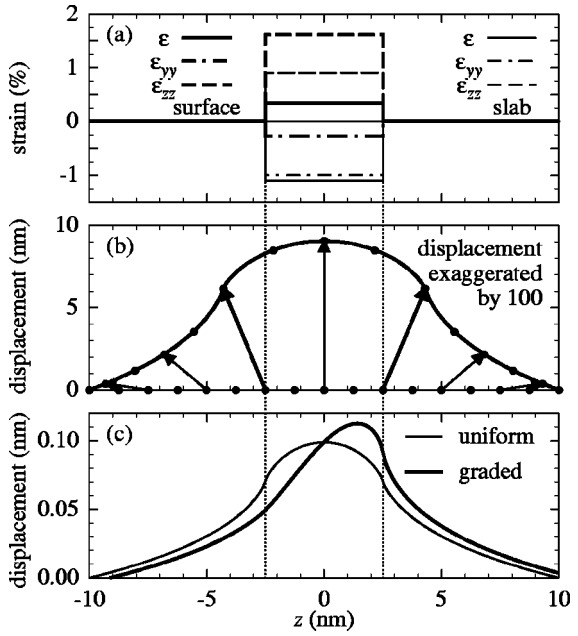

FIG. 2. Relaxation of the surface around the edge of a strained slab with width 5 nm and mismatch 1%. (a) Strains at surface (thick lines) and deep within the bulk (thin lines); (b) profile of surface with both components of displacement exaggerated by a factor of 100; (c) comparison of profile for a slab with uniform 1% mismatch (thin line) and one with mismatch graded linearly from 0% to 2% (thick line).

$$u_y(z)=C-\frac{2(1+\nu)\epsilon_0}{\pi}\left((z+a)\log\left|\frac{z+a}{a}\right|-(z-a)\log\left|\frac{z-a}{a}\right|\right). \tag{2}$$

An arbitrary constant C is present because the displacement does not decay at infinity, a pathological behavior of two-dimensional elasticity. This function is plotted in Fig. 2(b), where the displacement is exaggerated by a factor of 100 to emphasize both components of the relaxation. There is a logarithmic infinity in the slope of the edges of the slab, which may lead to artifacts in observations around these points.

The strains are shown as a function of depth, $-y$, for the middle of the slab ($z=0$) in Fig. 3(a). The change in sign of the dilation is clear. Neither tensile strain decays monotonically but has a minimum at a depth of $-y\approx a$. This is reflected in the displacement of the edge of the slab, plotted in Fig. 3(b). The slab relaxes to a greater thickness near the surface, as expected, but becomes *thinner* below this. All these functions decay only as $1/y$ and therefore persist to a large depth.

Carriers near the surface of the slab are particularly affected by the large strains. The changes in energy of the conduction band, light and heavy hole bands are given by[10]

$$\Delta E_c=a_c\epsilon, \quad \Delta E_{\mathrm{lh}}=a_v\epsilon+b_v\epsilon_{\mathrm{ax}},$$
$$\Delta E_{\mathrm{hh}}=a_v\epsilon-b_v\epsilon_{\mathrm{ax}}. \tag{3}$$

In these axes the axial strain $\epsilon_{\mathrm{ax}}=\epsilon_{zz}-\frac{1}{2}(\epsilon_{xx}+\epsilon_{yy})$, and the deformation potential constants for GaAs are $a_c=-7.5$ eV, $a_v=-0.4$ eV, and $b_v=-1.9$ eV. The dilation

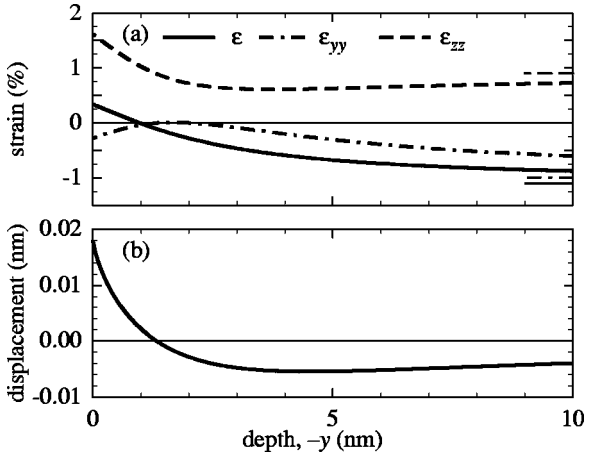

FIG. 3. Relaxation of strained slab as a function of depth, $-y$. (a) Tensile strains in middle of slab; (b) displacement of edge of slab showing a neck.

tends to trap electrons, holes, and excitons at the surface and may enhance the recombination velocity, although it is large for only a few nanometers near the surface. Heavy holes are also affected by the axial strain, which may trap them at $-y \approx a$. This has been observed in resonant tunneling diodes restricted to small pillars.[6]

The calculation is readily extended to a slab of nonuniform composition, where $\epsilon_0(z)$ acquires an arbitrary variation during growth. The strains at the surface are again given by Eq. (1) but are now proportional to the *local* value of $\epsilon_0(z)$. It is more convenient[9] to calculate the *slope* of the surface rather than its normal displacement directly:

$$\frac{du_y}{dz} = -2(1+\nu)\cdot\frac{1}{\pi}\int_{-\infty}^{\infty}\epsilon_0(s)\,\frac{ds}{z-s}. \tag{4}$$

This has the form of a Hilbert transform, as in the Kramers–Kronig relations, and can be inverted to give

$$\epsilon_0(z) = \frac{1}{2(1+\nu)}\cdot\frac{1}{\pi}\int_{-\infty}^{\infty}\frac{du_y}{ds}\,\frac{ds}{z-s}. \tag{5}$$

In both cases the principal part of the integral is understood. Thus it should be possible to deduce the composition of inhomogeneous layers from measurements of the slope of the distorted surface. This provides an alternative to the numerical modeling used to investigate strain induced by intermixing.[4]

An example of nonuniform composition is shown in Fig. 2(c), where the distortion of the cleaved surface is plotted for two wells of width 5 nm and the same average mismatch of 1%. The result for a uniform well given in Eq. (2) is compared with that for a graded well where the mismatch increases linearly from zero at $z=-2.5\,\mathrm{nm}$ to 2% at $z=+2.5\,\mathrm{nm}$. The difference could be measured by atomic force microscopy and used to study the variation of composition during growth, a common problem with materials that contain indium.

Another extension is to a well in a narrow mesa as shown in Fig. 1, rather than an infinitely thick wafer, which can again be solved using standard results in elasticity.[8] Cubic anisotropy can also be included analytically[11] but variable elastic constants would probably require numerical methods.

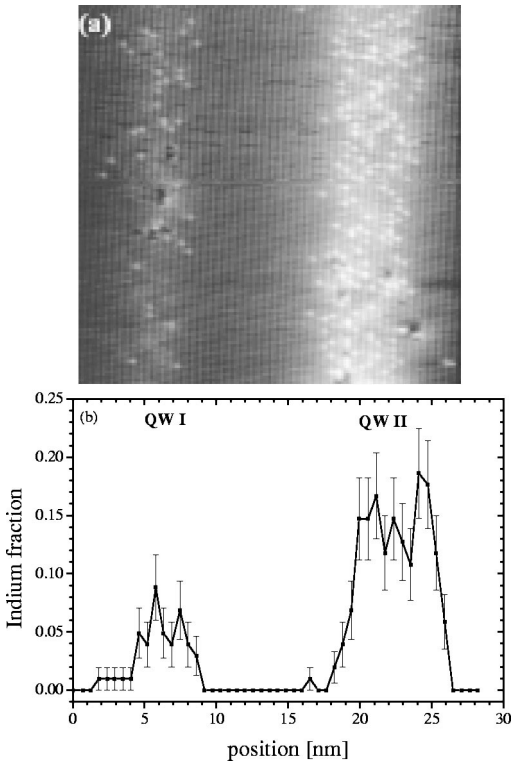

FIG. 4. (a) Atomic resolution, empty states, XSTM image of the double quantum well. The image was measured at an image voltage of 2.5 V and tunnel current of 0.198 nA, scan area $30\times30\ \mathrm{nm}^2$; (b) corresponding indium concentration profile derived from the XSTM image by counting indium atoms.

III. EXPERIMENT

A cleaved sample containing two InGaAs quantum wells, labeled QW I and QW II, within a GaAs matrix was investigated using cross-sectional scanning tunneling microscopy (XSTM). A typical scan is shown in Fig. 4(a). By choosing a positive or negative sample voltage with respect to the tip, which is grounded, it is possible to tunnel into the empty conduction band surface states [which are located at the group III elements for a cleaved (110) surface of III–V semiconductor crystals] or out of the filled valence band surface states (which are located at the group V elements). By measuring at the proper polarity of the tunnel voltage, it is thus possible to be sensitive to either the group III (positive voltages) or group V (negative voltages) elements in the top layer of the cleaved surface.

All measurements were performed under UHV conditions ($p<4\times10^{-11}\,\mathrm{Torr}$). The sample was cleaved *in situ* and the outward relaxation upon cleaving, due to the large built-in strain, was determined. From XSTM images with atomic resolution the width and the local indium concentration of the quantum wells can be determined, as shown in Fig. 4. Because of the difference in bond length and electrical properties of indium and gallium, the individual indium atoms can be distinguished from the surrounding GaAs ma-

TABLE I. Indium concentrations in the quantum wells determined by XSTM, XRD, and PL.

Well	Width (nm) XSTM	Indium concentration (%) XSTM	XRD	PL
QW I	4.5±0.5	5.0±0.5	5.2±0.5	6.3±0.5
QW II	6.5±0.5	14.4±0.6	13.7±0.5	14.7±0.6

trix in the STM images. By measuring at positive tunnel voltages (empty states imaging mode) the local indium fraction throughout the two quantum wells can be determined by counting the indium atoms. The results are shown in Fig. 4(b) shows that the indium content in the quantum wells can be considered to be constant within the accuracy of the measurement.

We compared our XSTM results concerning the determination of the composition of the quantum wells with two other standard techniques, photoluminescence (PL) and x-ray diffraction (XRD). The PL experiments were performed in a standard flow cryostat at 5 K using a diode pumped Nd:YAG laser operating at 25 mW at 532 nm and a backscattering configuration with a scanning spectrometer and a liquid nitrogen cooled CCD camera. The calculations were based on an effective mass approximation using parabolic bands and the solid-model theory of van de Walle[12] to calculate the band offsets between the different strained layers of the structure. The results of these measurements are shown in Table I. In the model used to interpret the PL and XRD spectra, the well width has to be inserted and was determined from the XSTM measurements. The estimates of the composition are in good agreement although PL tends to give a slightly higher concentration of indium.

The measured, apparent height of the cleaved quantum wells is determined both by the real outward relaxation and by contrast due to the different chemical properties (band gap, electron affinity, etc.) of the GaAs and InGaAs. The latter is sensitive to the magnitude and sign of the applied tunnel voltage. From height profiles shown in Fig. 5(a), the ''apparent relaxation'' of the InGaAs QW II with respect to the surrounding GaAs matrix is determined at different tunnel voltages, and plotted as a function of voltage in Fig. 5(b).

The apparent relaxation in the profiles obtained from filled states images (negative tunnel voltage) is almost independent of the image voltage. In the empty states images (positive tunnel voltage), however, there is a strong voltage dependence and at low tunnel voltages there is a large electronic contrast. This is due to the fact that in filled states imaging the relative tunnel barrier height difference between the GaAs and the InGaAs with respect to the the vacuum barrier is much smaller than in the empty states imaging mode, resulting in a very weak voltage dependence of the tunnel current (and thus the measured height differences) due to differences in chemical composition.[13] At high tunnel voltages the measured relaxation profiles approach a constant value, independent of the polarity of the applied tunnel voltage. In order to determine only the real outward relaxation and suppress the electronic contrast, XSTM measurements should be performed at high positive tunnel voltages (empty states) or negative tunnel voltages (filled states imaging).

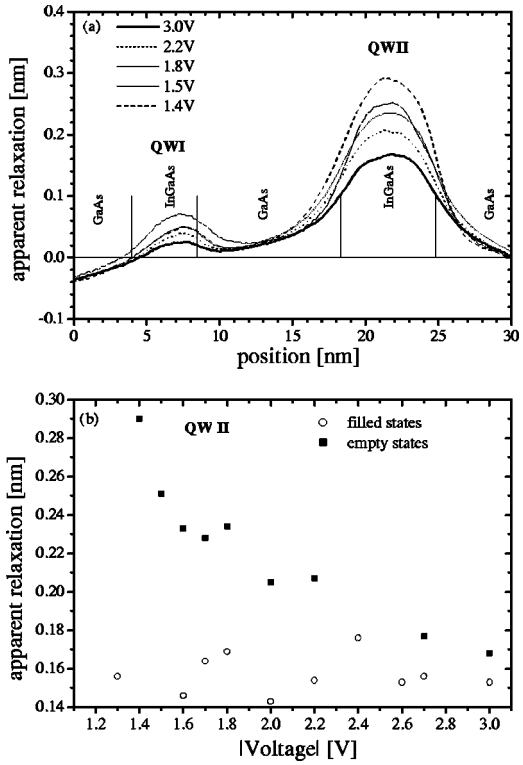

FIG. 5. (a) Apparent outward relaxation profile of the double quantum well at different positive tunnel voltages (empty states mode imaging); (b) apparent outward relaxation height of QW II as a function of tunnel voltage.

The lattice constant can be determined from Fig. 4(a) by measuring the distance between the atomic rows. To get an accurate value, some averaging of the local indium fluctuations is necessary, which can be done by Fourier filtering perpendicular to the growth direction. The measured lattice constant profile is shown in Fig. 6. The lattice constant changes abruptly at the interfaces between the quantum wells and the surrounding GaAs matrix and the value of the lattice constant throughout the quantum wells can be considered to be constant. This is good qualitative agreement with the calculations. Numerical agreement, however, requires a higher indium concentration in the calculation than that deduced from the XSTM measurements: 7% and 17.1% instead of 5%

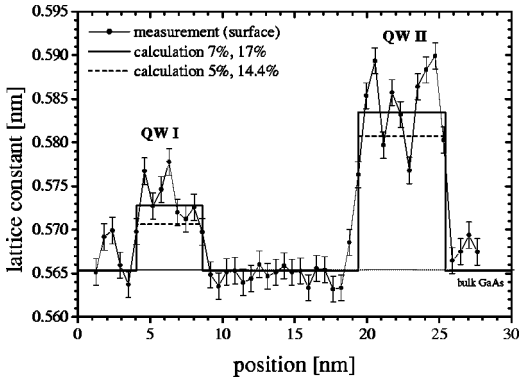

FIG. 6. Lattice constant profile at the cleavage plane obtained from atomic resolution XSTM images.

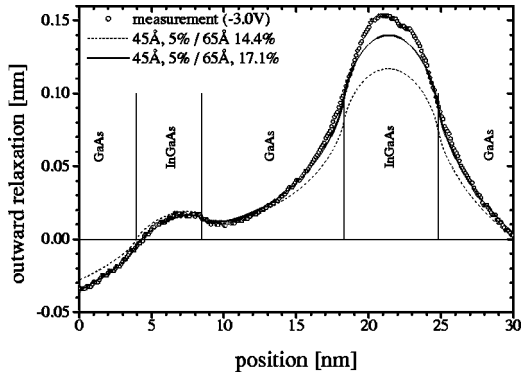

FIG. 7. Outward relaxation profile of the double quantum well, compared with calculations of the outward relaxation. Image voltage −3.0 V, current 0.110 nA.

and 14.4%. Thus the calculation appears to predict too small a distortion of the surface. The measured lattice constant of the GaAs however, exactly agrees with the theoretical value, confirming that the STM is calibrated properly.

In Fig. 7, the measured outward relaxation with minimal electronic contrast is compared with calculations. The overall shape of the calculated profile is again qualitatively consistent with the measured relaxation profile. Once more, however, the measurement indicates a stronger outward relaxation than the profile calculated with the use of the indium concentrations found from the XSTM measurements. A better fit can again be achieved by using an increased indium concentration of 17.1% for QW II.

IV. DISCUSSION

Agreement is good between the theory and experiments at a qualitative level. The prediction that the lattice constant of the GaAs should be unaffected on the surface, while that of the quantum well is changed by a constant factor, is strongly supported. Similarly, the shape of the outward distortion of the cleaved surface is described well. The disagreement is in the magnitude of the distortion, with the calculation predicting about 80% of that measured in the experiments. We now consider some possible reasons for this discrepancy.

First, it could be possible that the XSTM measurements are unrepresentative of the bulk because of artefacts arising from cleavage, for example, the desorption of indium. Against this we note the good agreement between the three determinations of the indium concentration summarized in Table I and the fact that no defects or vacancies are observed in the XSTM images. It also seems unlikely that the estimate of the width is influenced by the extreme slope of the surface at the edges of the well [Eq. (2)]. The problem probably lies in the way a cleaved surface behaves, the way it is imaged during the STM measurements, or in one of of the assumptions on which the calculation is based.

(1) During filled states imaging, only the arsenic lattice is visible in the STM images and the indium atoms in the top layer of the cleaved surface are therefore not visible. However, an indium atom in the second layer, which is much larger than a gallium atom, will push up the arsenic atom in the top surface layer by about 16 pm in the STM images. This will give an increase of the measured relaxation profile in the quantum well, which is not included in the calculation.

(2) When a (110) surface of a III–V semiconductor is cleaved the surface reconstruction and buckling angle of the surface depend on the composition of the cleaved layer. The resulting reconstruction of the arsenic lattice is 10–20 pm larger for a cleaved InAs surface than for a GaAs surface.[14] This again will give an extra increase in the measured relaxation profile of the quantum wells during filled states imaging.

(3) The effects mentioned in 1 and 2 are given for pure InAs and GaAs. When considering a layer with an indium content of about 17% the resulting total extra measured outward relaxation in QW II will be about 6 pm. When including this in the calculation, a much better fit with the calculated 17.1% indium content profile is obtained, especially inside the actual quantum well region. This is, however, still in disagreement with the indium content of 14.4%, which not only has been determined locally by STM, but also by techniques that determine the average indium concentration on a larger scale, PL and XRD.

(4) It has been assumed that the elastic constants are the same throughout the sample, but InAs is considerably less stiff than GaAs. At first sight this might be expected to make the calculated deformation larger, but the opposite is the case. The reason is that the applied pressure P depends on the elastic constants of the *well*. Thus a less stiff well leads to a lower force, and the displacement is reduced by the stiffer cladding layers.

(5) The theory is for isotropic elasticity but the materials are cubic. An analytic calculation is possible[11] but we have not yet attempted it. The expression for the pressure required to force the well to match the cladding layers becomes $P=\epsilon_0 E/(1-\nu)=\epsilon_0(s_{11}+s_{12})$ in a cubic material. We have used a value of Poisson's ratio consistent with this, $\nu=-s_{12}/s_{11}=0.31$ for GaAs, and P therefore already has its correct value allowing for cubic symmetry. This is an extreme value of ν, however, and an angular average might be more appropriate when calculating the subsequent relaxation at the cleaved surface. The result is $\langle\nu\rangle\approx 0.25$, which would *reduce* both the strain in the plane of the surface and the displacement according to Eqs. (1) and (2).

(6) We have assumed that the linear theory of elasticity can be used, but the strains of over 1.5% may render this invalid. Unfortunately we are not aware of any calculations that employed nonlinear elasticity. The crucial feature would be an enhanced value of P to increase the distortion. Nonlinearity would be strongest very near to the surface and would therefore have a smaller effect on $u_y(z)$, which depends on the integral over strain as a function of depth. The similarity between the errors in $\epsilon_{zz}(z)$ and $u_y(z)$ is evidence against significant nonlinearity.

(7) There may be forces at the interfaces between GaAs and InAs, and at the exposed surface, as a result of interface and surface energies. Any such forces would have to be significant compared with $2\ Pa\approx 8\ \mathrm{Nm}^{-1}$.

(8) Finally, we have neglected piezoelectric effects.[15] The coupling is weak enough that there should be no signifi-

cant effect on the elastic field itself, but the piezoelectric potential could influence the STM. Against this, it seems unlikely that the lattice constant in the plane of the surface would be affected.

We are unable to explain the discrepancy at present but plan to investigate the effect of different elastic constants and cubic symmetry more carefully.

V. CONCLUSIONS

A simple method has been described for calculating the elastic field around a strained quantum well at a cleaved surface and compared with cross-sectional scanning tunneling microscopy. The normal displacement may be particularly useful for interpreting atomic force microscopy at lower resolution and an integral transform can be used to recover the variation of composition from measurements of the slope of the surface.

The strain in the plane of a cleaved surface and the normal displacement have been measured by XSTM for a sample containing two InGaAs quantum wells in GaAs. The composition of the wells was determined by counting indium atoms on the surface and confirmed by x-ray diffraction and photoluminescence. Qualitative agreement between the measured distortion of the surface and the calculations is good. The strain in the plane of the surface is found to be constant within a well and vanishes in the cladding, as predicted by the theory, and the shape is also consistent. However, the calculations predict only about 80% of the displacement directly measured by XSTM. This discrepancy can be partly explained by the larger size of the indium atoms and the different buckling behavior and surface reconstruction upon cleavage, which cause a different relaxation behavior of the GaAs and InGaAs layers. We have been unable to determine the reason for the remaining discrepancy, although the assumption of isotropic symmetry in the calculation seems most likely.

ACKNOWLEDGMENTS

The authors would like to thank Tom Eijkemans for performing the XRD and PL measurements. This work was financially supported by QUEST, a National Science Foundation Science and Technology Center, Grant No. DMR 91-20007, by the Leverhulme Trust (UK), and by the Joint Research Program of the Netherlands Organization for Scientific Research (NWO) and the British Council. J.H.D. is grateful for conversations with D. R. Clarke.

[1] P. G. Piva, R. D. Goldberg, I. V. Mitchell, H. Chen, R. M. Feenstra, G. C. Weatherly, D. W. McComb, G. C. Aers, P. J. Poole, and S. Charbonneau, Appl. Phys. Lett. **72**, 1599 (1998).
[2] B. Legrand, B. Grandidier, J. P. Nuys, D. Stiévenard, J. M. Gérard, and V. Thierry-Mieg, Appl. Phys. Lett. **73**, 96 (1998).
[3] H. Chen, R. M. Feenstra, R. S. Goldman, C. Silfvenius, and G. Landgren, Appl. Phys. Lett. **72**, 1727 (1998).
[4] H. Chen, R. M. Feenstra, P. G. Piva, R. D. Goldberg, I. V. Mitchell, G. C. Aers, P. J. Poole, and S. Charbonneau, Appl. Phys. Lett. **75**, 79 (1999).
[5] T. Pinnington, A. Sanderson, T. Tiedje, T. P. Pearsall, E. Kasper, and H. Presting, Thin Solid Films **222**, 259 (1992).
[6] C. D. Akyüz, A. Zaslavsky, L. B. Freund, D. A. Syphers, and T. O. Sedgwick, Appl. Phys. Lett. **72**, 1739 (1998).
[7] M. Y. He, J. Lipkin, D. R. Clarke, A. G. Evans, and M. Tenhover, Acta Mater. **44**, 2353 (1996).
[8] S. P. Timoshenko and J. N. Goodier, *Theory of Elasticity* (McGraw-Hill, New York, 1970), Sec. 148.
[9] K. L. Johnson, *Contact Mechanics* (Cambridge University Press, Cambridge, 1985), Sec. 2.5. Note that Johnson takes the force *P* inward, while it is outward here to match the measurements.
[10] See, for example, E. P. O'Reilly, Semicond. Sci. Technol. **4**, 121 (1989).
[11] A. E. Green and W. Zerna, *Theoretical Elasticity* (Oxford University Press, Oxford, 1968), Chap. 9.
[12] C. G. van de Walle, Phys. Rev. B **39**, 1871 (1989).
[13] D. M. Bruls, P. M. Koenraad, M. Hopkinson, J. H. Wolter, and H. W. M. Salemink, Appl. Surf. Sci. (in press).
[14] W. Mönch, *Semiconductor Surfaces and Interfaces*, 3rd ed. (Springer, Heidelberg, 2001), Chap. 7.
[15] J. H. Davies, D. E. Petticrew, and A. R. Long, Phys. Rev. B **58**, 10789 (1998).